Numerical analysis of reinforced concrete continuous deep beams

Melvin Asin and Joost Walraven
Delft University of Technology. Faculty of Civil Engineering, Section of Concrete Structures

The structural behaviour of deep beams is still not completely understood, since, for example, plane sections do not remain plane and no uniform shear flow can develop because of the small ratio between depth and shear span. If in addition, the supporting system is also statically indeterminate, the number of difficulties increases. In order to investigate the behaviour of statically indeterminate deep beams, a series of fourteen tests has been carried out. Variables were the slenderness, the ratio between top and bottom reinforcement, and the amount of shear reinforcement.
Complementary to these experiments numerical simulations have been carried out. This paper focuses on the computational aspects. A good match between experimental behaviour and numerical simulation was found over the entire range, which increases the confidence in the predictive capacity of non-linear finite element analysis.
Extrapolation was the next step: calculations were made for cases in which either a material or a structural parameter was varied beyond the tested range.
For this study, the amount of compressive strength reduction by transverse tension was chosen as a material parameter. In general this appeared to have a negligible effect on the behaviour. Only in the case of large reductions, however, a change in failure mechanism and a decrease in failure load were found.
The orientation and the amount of web reinforcement was chosen as a structural parameter. Compared to the original calculation with vertical reinforcement only, a decrease in failure load is found when only horizontal web reinforcement was present. A combination of both horizontal and vertical reinforcement proved to be the most effective: at the expense of more reinforcement, it resulted in a strength increase as well as in small crack widths.

Keywords: **experiments, non-linear finite element analysis, continuous deep beams, compressive strength reduction, web reinforcement.**

1 Introduction

The structural behaviour of continuous deep beams is not completely understood. The behaviour of deep beams differs from that of slender beams, due to the characteristic small ratio between shear span and depth. In contrast to slender beams, the response is characterized by non-linear strain distributions (even in the elastic stage), and a significant direct load transfer from the point of loading to the supports. Furthermore, continuous deep beams are highly sensitive to imposed deformations, such as differential support settlements, because of their large bending stiffness.

HERON, Vol. 40, No. 2 (1995) ISSN 0046-7316

In simply supported deep beams that are subjected to concentrated loads, two load bearing mechanisms can generally be recognized, namely: strut-and-tie action (bottom flexural reinforcement) and truss action (shear reinforcement and flexural reinforcement). However, the structural behaviour of continuous deep beams becomes more complicated, since an extra load bearing mechanism is introduced, namely: additional strut-and-tie action (by top flexural reinforcement), see Figure 1. The sum of the contributions of all these three mechanisms must balance the applied load. The ratios between the individual contributions are yet unknown. In fact these mechanisms influence each other and are furthermore dependent on differences in their stiffness, as caused e.g. by cracking. Even recent codes do not give clear design recommendations on these matters. For instance, EuroCode (1991) only states that "*deep beams under concentrated loads may be designed using a simple strut-and-tie model*" (2.5.3.7.3(1)), and that "*in some cases, e.g. lower depth/span ratios, distributed loads, more than one concentrated load, etc., models combining strut-and-tie action with truss action may be used*" (2.5.3.7.3(2)). How that should be done remains unclear, although it is essential for design purposes to correctly estimate the expected contributions of the various load bearing mechanisms in order to design and detail correctly.

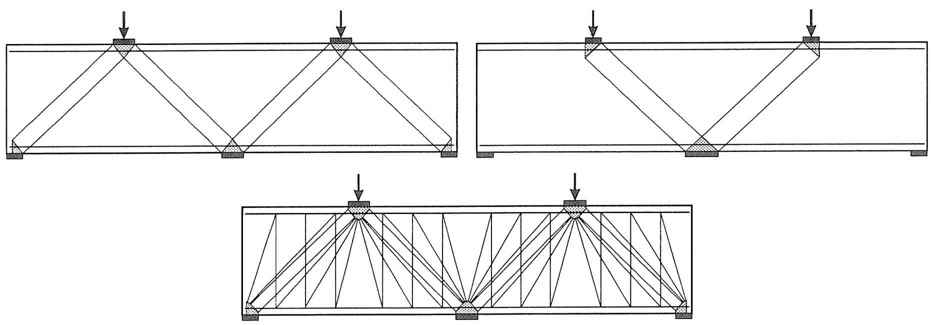

Fig. 1. Load bearing mechanisms in continuous deep beams: strut-and-tie action with bottom reinforcement, strut-and-tie action with top reinforcement, combination of strut-and-tie action with truss action.

2 Experiments

To extend the knowledge on behaviour and to develop better design models for continuous deep beams, an experimental program was conducted at the Stevin laboratory of the Delft University of Technology, see Asin (1992). Fourteen large-size two span beams were tested. The slenderness ratio, the ratio of top and bottom flexural reinforcement and the vertical web reinforcement ratio were selected as the main variables. The parameters were chosen in such a way that the contributions of any of the three load bearing mechanisms were varied.

The specimen code can characterized as BM A/B/C, in which "A" represents the (a/d)-ratio, "B" the ratio of top and bottom flexural reinforcement and "C" the amount of vertical web reinforcement. Table 1 shows details of the used reinforcement. An example of the geometry and the reinforcement layout is shown in Figure 2.

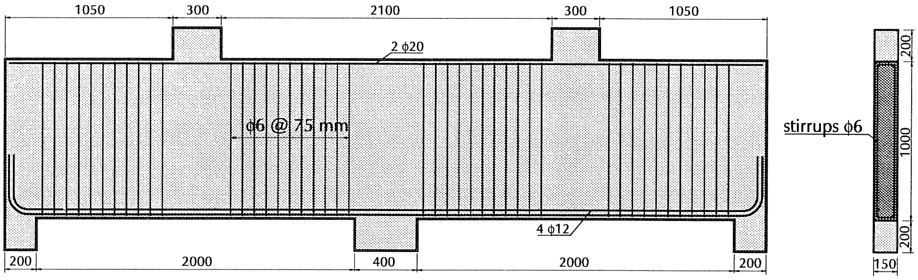

Fig. 2. Typical geometry and reinforcement layout: BM 1.0/1/1.

The specimens were cast vertically. The specimens, two span beams, which were symmetrical with regard to the middle support, were loaded at mid span. To ensure an uniform introduction of loads and reactions monolithic concrete column stubs were provided.

Table 1. Reinforcement used.

Specimen Code	Top Reinforcement	Bottom Reinforcement	Vertical Web Reinforcement
1.0/1/1(r)	2 φ 20 [628 mm^2]	4 φ 12 [452 mm^2]	11 φ 6 @ 75 mm
1.0/1/2			8 φ 6 @ 100 mm
1.0/1/3			5 φ 6 @ 170 mm
1.0/2/1	4 φ 12 [452 mm^2]	2 φ 20 [628 mm^2]	11φ 6 @ 75 mm
1.0/2/2			8 φ 6 @ 100 mm
1.0/2/3			5 φ 6 @ 170 mm
1.5/1/1	2 φ 20 + 2 φ 10 [785 mm^2]	2 φ 20 [628 mm^2]	11φ 6 @ 75 mm
1.5/1/1*			6 φ 8 @ 140 mm
1.5/1/2			8 φ 6 @ 100 mm
1.5/1/3			5 φ 6 @ 170 mm
1.5/2/1	2 φ 20 [628 mm^2]	2 φ 20 + 2 φ 10 [785 mm^2]	11 φ 6 @ 75 mm
1.5/2/2			8 φ 6 @ 100 mm
1.5/2/3			5 φ 6 @ 170 mm

The specimens were tested in a load-controlled manner until failure, in which the loads were applied by two manually operated hydraulic jacks. The specimens were heavily instrumented to obtain as much data as possible. The measurements included: loads and reactions, crack patterns, steel strains, and overall and local deformations.

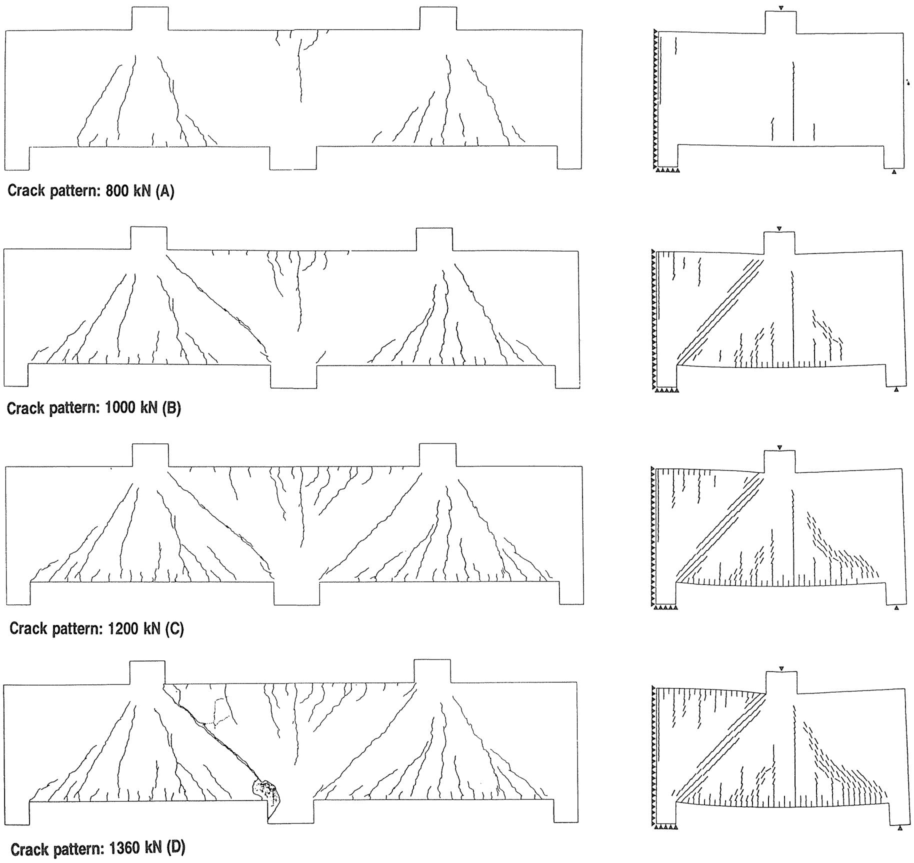

Fig. 3. Crack pattern development in BM 1.0/2/3, as observed experimentally (left) and as simulated (right).

The characteristic structural behaviour of continuous deep beams can best be explained by the development of the crack pattern. An example is shown in Figure 3 (BM 1.0/2/3).
Flexural cracking starts at mid span. This typically occurs at a total load (= sum of the two jack loads) of approximately 400–600 kN. Flexural cracking over the supports occurs at a later stage (total load 800 kN, Figure 3A). The sequence of crack formation is contrary to predictions by the slender beam theory, which predicts that flexural cracking starts over the supports. This discrepancy is ascribed to the effects of shear deformations. Shear cracking occurs at a load level of 900–1100 kN (Figure 3B). After the formation of shear cracks, a substantial load increase is still possible

dependent on the amount of stirrups. At this stage secondary flexural cracking occurs (Figure 3C). Ultimately a brittle shear failure is found (Figure 3D). This is accompanied by crushing of the concrete in the load and support regions, and yielding and consequently fracturing of the shear reinforcement.

3 Simulations

The experimental behaviour of the test specimens was simulated with the non-linear finite element program SBETA, Cervenka et al. (1990); Cervenka et al. (1992, 1993). This plane stress analysis uses the smeared crack approach with the fixed crack model.

The following constitutive relations are available in SBETA:
In concrete under compression a parabolic stress-strain law is used and a linear behaviour is assumed in tension prior to cracking (Figure 4, left). Peak stresses are taken from Kupfer's failure envelope. Post-peak softening is considered in compression and tension.

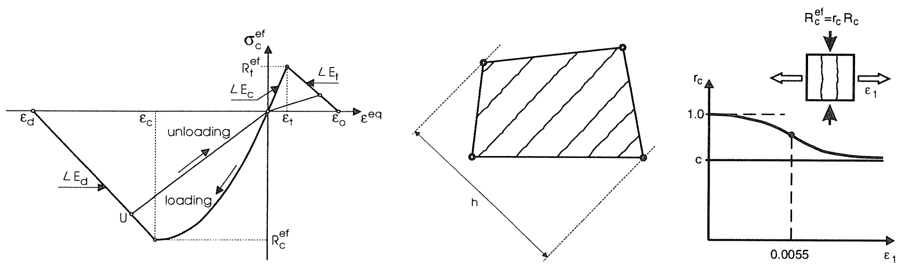

Fig. 4. Constitutive model in SBETA: (left) stress-strain law, (middle) crack band calculation, (right) peak stress softening.

Non-linear fracture mechanics is introduced by means of the crack band theory (Bažant et al. (1983)). The crack band is derived from the actual crack direction and the element orientation as a projection of the largest element size normal to the crack direction (Figure 4, middle). The tensile softening curve can either be linear or according to Hordijk et al. (1990). The compressive peak stress reduction of the cracked concrete as a function of the lateral strain is considered similarly to the model of Vecchio et al. (1983), in which the amount of the reduction *c* is chosen by the user (Figure 4, right). The shear retention factor can either be a function of the lateral strain (Kolmar (1985)) or a constant value.
The stress-strain law for the reinforcement is assumed to be bilinear. Perfect bond is assumed. Furthermore, tension stiffening may explicitly be modelled by inclusion of a tension stiffening stress σ_{ts}.

Since the test specimens are symmetrical, only (the right) half of the beam was modelled, taking the centreline of the middle support as the axis of symmetry. For analysis 632/1016 four-noded quadrilateral elements were used for the specimens with (a/d)=1.5/1.0 respectively. The reinforcement was modelled as being both discrete (flexural reinforcement), and smeared (shear reinforcement).

The properties determined in the standard tests on concrete cubes (150 × 150 × 150 mm) and prisms (400 × 150 × 150 mm) were used as input parameters in the numerical analysis (see Table 2). Figure 4 explains the used symbols. The compressive strength was taken to be 85% of the average cube strength, whereas the tensile strength was assumed to be equal to 75% of the average splitting strength. For the fracture energy G_F a value of 125 N/m was taken: this value ensured good agreement between experimental and numerical elongations of the tension ties. The Young's modulus used was determined by standard tests on prisms. The yielding and tensile strengths of the reinforcement were obtained from standard tensile tests of reinforcing steel.

Table 2. Input parameters for non-linear analysis.

Specimen Code	R_c [MPa]	R_t [MPa]	E_c [MPa]
1.0/1/1	26.8	1.87	35100
1.0/1/2	27.5	1.89	35400
1.0/1/3	25.8	1.88	34700
1.0/2/1	25.2	1.59	35100
1.0/2/2	28.2	1.84	38600
1.0/2/3	30.4	2.12	38500
1.5/1/1	29.6	1.87	37800
1.5/1/1*	29.9	1.97	37200
1.5/1/2	28.9	2.00	34600
1.5/1/3	25.9	1.95	33100
1.5/2/1	27.8	1.92	33900
1.5/2/2	26.0	1.88	34400
1.5/2/3	28.5	1.91	36200

Unless explicitly stated otherwise, the concrete was modelled as follows: the fixed crack model and a Poisson's ratio of 0.2 were used, tensile softening according to Hordijk et al. (1990) was taken into account, the compressive peak stress reduction was neglected (c = 1.0), the variable shear retention factor was used, and explicit tension stiffening was not taken into account.
The following yield strengths were determined for the reinforcing bars: f_{sy} ϕ (6-12–20 mm) = (569–586–567) MPa. Young's modulus was taken as 210 GPa, whereas the hardening moduli for bars ϕ (6–12–20 mm) equalled (8.1–44.5-36.0) GPa.

As has been shown previously (Asin et al. (1994)), the development of the crack pattern of BM 1.0/1/3 was well predicted, which indicates that the structural response was accurately simulated. The load-deflection and the load-reaction curves were also predicted with sufficient accuracy.
The above mentioned criteria of comparison relate to the overall behaviour. Furthermore, it was shown in the same publication that the local behaviour was also correctly simulated. This was illustrated by the predicted change in load transfer within the inner shear span caused by shear cracking. The prediction was in excellent agreement with the experimental observations.

The predictive capacity of the numerical analysis with regard to crack pattern development is again shown in Figure 3, in this case for BM 1.0/2/3. The shown load levels correspond to the sum of the jack loads. Good agreement between experiment and simulation is found at various stages of loading. The examples mentioned above all refer to specimens with an (a/d)-ratio of 1.0.

To verify whether the behaviour of more slender specimens ((a/d) = 1.5) can also be predicted accurately, load deflection responses of BM 1.5/1/3 and BM 1.5/2/1 are shown in Figure 5. The two experimental curves represent the deflections of the two loading columns.
Both specimens have the same slenderness, but differ in reinforcement layout and in the amount of shear reinforcement. The resulting curves of the experiments and the simulations match excellently.

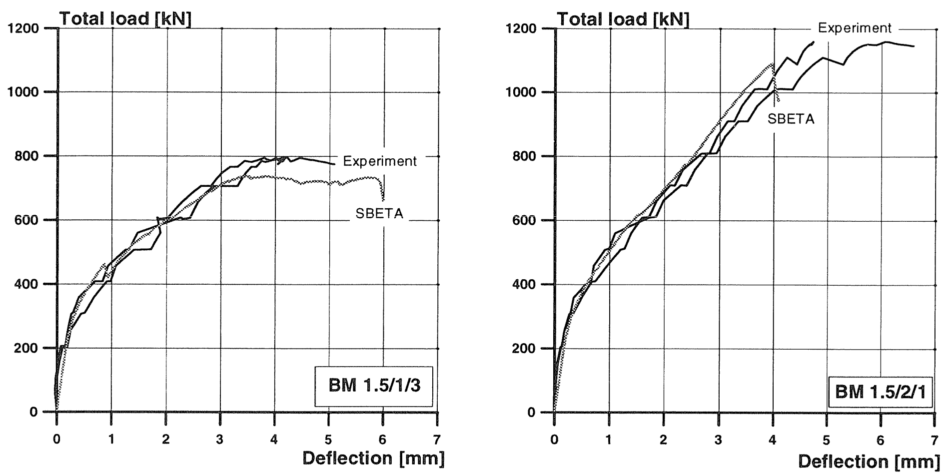

Fig. 5. Calculated load-deflection diagrams for (a/d) = 1.5: BM 1.5/1/3 (left) and BM 1.5/2/1 (right).

Finally, Figure 6 shows the experimental and the numerical shear capacity as a function of the shear reinforcement ratio ω_{ss}. The ratio of the experimental and the numerical shear strength has an average value of 1.03 and a standard deviation of 14% for the test series.

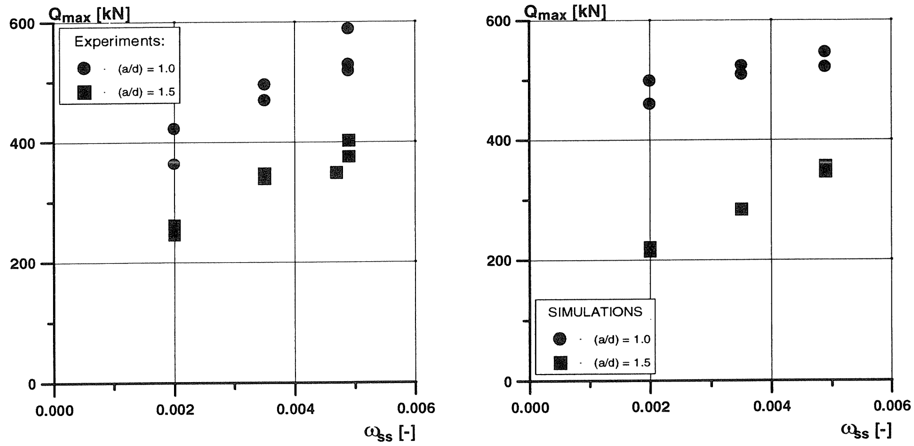

Fig. 6. Shear capacity as a function of the shear reinforcement ratio ω_{ss}: experimental (left) and numerical (right).

An overview of the simulations shows good agreement between experiments and simulations. Since this proves the reliability of the non-linear finite element analysis a next step could be initiated. A study was carried out into the influence of parameter variations, both within and outside the range of experiments.

4.1 *Compressive strength reduction by transverse tension*

There has been much debate on the effect of a reduction of the compressive stress due to transversal tensile strains.
The discussion focuses on three aspects: (1) whether a reduction of the compressive stress due to transversal tensile strains really exists, Feenstra (1993), (2) if so, what is the maximum amount of stress reduction, Kollegger et al. (1990), and (3) how should this be taken into account, Vecchio et al. (1993).

Compressive strength reduction by transverse tension is considered to be an important item: in non-linear finite element analysis of continuous deep beams it was stated to be *essential* that the constitutive model for concrete should account for it, Rogowsky (1990).
Continuous deep beams are structures that are characterized by zones with high compressive stresses from the point of loading to the supports. In the inner shear span of continuous deep beams these compressive zones are crossed by zones with high tensile strains. Both the experiments and the simulations showed failure by crushing of the concrete after the compressive strength had been exceeded. It was expected that a reduction of the compressive strength, for instance as caused by transversal tensile strains, would be detrimental to the bearing capacity of the structure.
This mechanism is taken into account in the Canadian Code (1984).

In the SBETA program the user-defined variable (c) controls the ratio between the reduced and the original compressive strength. In the previous calculations no reduction of the compressive strength was used ($c = 1.0$).
Three additional computations were made with $c = 0.8/0.6/0.4$ respectively. Specimen BM 1.0/1/3 was selected, because it was considered to be the most critical. As this specimen has minimum shear reinforcement, this should lead to the highest tensile strains and the largest reductions of the compressive strength. The results are shown in Table 3 and Figures 7–9.

Figure 7 shows the calculated load-deflection responses with varying amounts of compressive strength reduction. It is very clear that the overall structural response is not influenced, with the exception of the peak load.

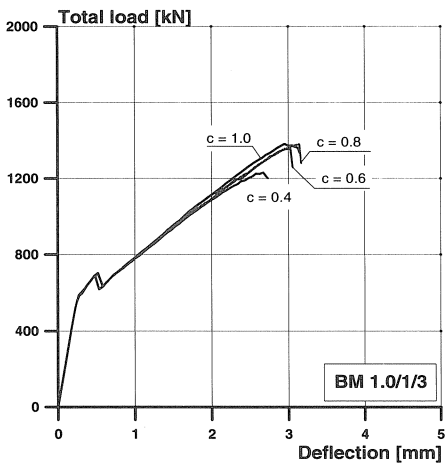

Fig. 7. Load-deflection diagrams for BM 1.0/1/3 with varying amounts of compressive strength reduction.

Table 3. Peak loads - shear forces with varying amounts of compressive strength reduction (BM 1.0/1/3).

Reduction factor	P_{max}	Q_{max}
$c = 1.0$	691	460
$c = 0.8$	679	454
$c = 0.6$	690	457
$c = 0.4$	615	406

Figure 8 shows the isolines for principal compressive stresses for the two extreme cases, namely (c = 1.0) and (c = 0.4). The plots refer to a total load level of 1100 kN. Although the case with (c = 1.0) does show a more condensed compression strut, the differences are small. Plots with isolines for principal strains, either tensile or compressive, give the same results.
Even this rather extreme variation in reduction of the compressive stress does not lead to significant changes in the internal load transfer in the inner shear span.

However, a change in failure mechanism is observed (Figure 9). As the reduction of the compressive strength increases, the regions in which crushing of concrete occurs (the grey shaded areas) shift from the load introduction areas towards mid span.
Figure 9 (left) shows the final (post peak) stage for (c = 1.0): failure due to crushing occurs in the regions near the supports and the load introduction. Figure 9 (right) shows the ultimate stage for (c = 0.4). Now the peak load is associated with crushing in the interior of the web. This shift only occurs with a *large* compressive strength reduction.

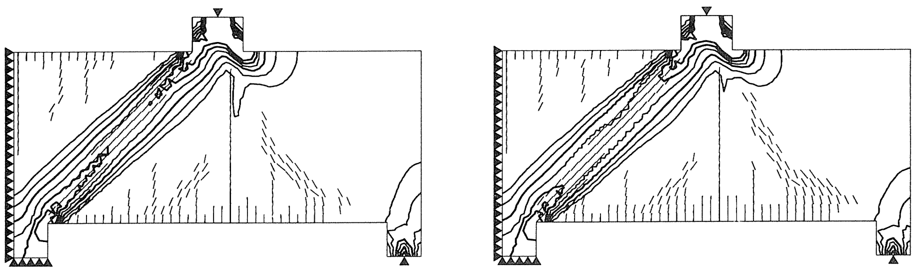

Fig. 8. Isolines for compressive stresses for BM 1.0/1/3, load level: 1100 kN: (left): c = 1.0, (right): c = 0.4.

gure 8: Isolines for compressive stresses for BM 1.0/1/3, load level: 1100 kN: (left): c= 1.0, (right): c = 0.4

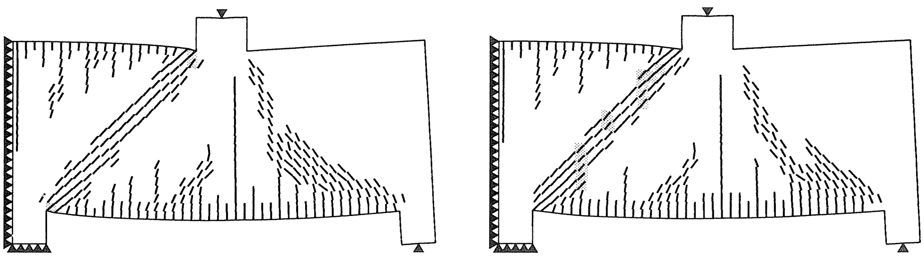

Fig. 9. Crack pattern at failure for BM 1.0/1/3: (left): c = 1.0, peak load: 1381 kN, (right): c = 0.4: peak load: 1230 kN.

The main conclusion is that the reduction of the compressive strength due to transversal tensile strains hardly affects the structural behaviour of reinforced concrete continuous deep beams, in

spite of the fact that there is a large region in which compressive stresses and large transversal tensile strains are found. No large differences can be detected in the load-deflection curves, nor in the load distribution in the inner shear span for the range investigated.
The reason is that mesh elements under critical stress conditions are hardly affected by the possible stress reduction. Firstly, the elements near the load introduction zones either develop only small tensile strains, or they remain in a biaxial compressive state of stress. As a result the compressive strength is hardly reduced. Secondly, the elements at mid span do undergo large tensile strains and consequently a reduction of the compressive strength. However, due to the fanning of compressive stresses in the web the stress levels in that area are not critical anymore.

4.2 *Amount and orientation of web reinforcement*

Another point worth investigating is whether a horizontal or a vertical arrangement of web reinforcement is the most effective way to enhance the shear strength of deep beams. There still remain questions on this aspect.
There is experimental evidence that indicates that the use of horizontal web reinforcement is not very effective in increasing the shear strength in deep beams, Kong et al. (1970), Smith et al. (1982), Rogowsky et al. (1983), Lehwalter (1988). It was concluded that only vertical web reinforcement is beneficial in that respect. However, the results seem to depend on the slenderness ratio: Smith et al. (1982) and Kong et al. (1970) report that the effect of vertical web reinforcement on the ultimate shear strength diminishes for small (a/d)-ratios. Mau et al. (1987) come to the same conclusion after a theoretical study. Additionally, Smith et al. (1982) and Kong et al. (1970) report that horizontal web reinforcement becomes increasingly more effective for small (a/d)-ratios than vertical web reinforcement.
These results should be cautiously applied to continuous deep beams, since most of the test results concern simply supported beams. In this respect it is worthwhile to note that whereas the American Code (1989) regards horizontal web reinforcement effective to increase the shear strength of *simply supported* deep beams, it does not consider it effective to increase the shear strength of *continuous* deep beams.

When these experiments were prepared the choice was made to use vertical instead of horizontal web reinforcement (Asin (1992)), because it was expected that vertical reinforcement would be more efficient in increasing the shear strength. A combination of both horizontal and vertical web reinforcement was not considered, because the aim was to isolate the influence of the type of web reinforcement on the shear strength. Non-linear finite element analysis provides a tool to validate the made choice, and more general, to investigate the effectiveness of web reinforcement to increase the shear strength of continuous deep beams (depending on the orientation and the amount of reinforcement).
For this purpose three specimens were selected, namely: BM 1.0/1/1(r), BM 1.0/1/2 and BM 1.0/1/3. All had an (a/d) ratio of 1.0, and a layout of the longitudinal reinforcement calculated on the basis of the theory of elasticity. The specimens did have different amounts of vertical web

reinforcement, with BM 1.0/1/1 (r) having maximum and BM 1.0/1/3 having minimum stirrups respectively (see also Table 1).
The original calculations were simulations of the experiments (vertical web reinforcement only). For each specimen two additional calculations were made: (1) with the same ratio of web reinforcement, but now only horizontal, and (2) with the same ratio of web reinforcement, but now both horizontal and vertical. Web reinforcement was only placed in the shear span. The used reinforcement scheme is shown in Table 4. The other input parameters remained unchanged.

Table 5 shows that for these geometries, a horizontal web reinforcement reduces the ultimate capacity in comparison with the original calculation with a vertical web reinforcement only.
A combination of both horizontal and vertical reinforcement is the most effective way to increase the shear strength and leads to the highest failure loads, albeit at the expense of twice as much reinforcement. These tendencies are consistent with the experimental observations of e.g. Lehwalter (1988) and Rogowsky et al. (1983), and validate the choice made in the experimental programme.

Table 4. Overview used reinforcement schemes.

	Only vertical (original)		Only horizontal		Horizontal & Vertical	
Specimen Code	ρ_v [-]	ρ_h [-]	ρ_v [-]	ρ_h [-]	ρ_v [-]	ρ_h [-]
1.0/1/1 (r)	0.0049	–	–	0.0049	0.0049	0.0049
1.0/1/2	0.0035	–	–	0.0035	0.0035	0.0035
1.0/1/3	0.0020	–	not calculated		0.0020	0.0020

Table 5. Calculated peak loads and corresponding shear forces.

	Only vertical (original)		Only horizontal		Horizontal & Vertical	
Specimen Code	P_{max}	Q_{max}	P_{max}	Q_{max}	P_{max}	Q_{max}
1.0/1/1 (r)	813	546 [0.672 P]	603	386 [0.639 P]	914	599 [0.655 P]
1.0/1/2	763	509 [0.668 P]	564	359 [0.637 P]	810	532 [0.656 P]
1.0/1/3	691	460 [0.666 P]	not calculated		668	438 [0.655 P]

Figure 10 presents the calculated load-deflection response for BM 1.0/1/1 (r) with varying orientation of web reinforcement: horizontal, vertical and both.
The orientation of the web reinforcement influences the response. After shear cracking, the beam with horizontal reinforcement only responds stiffer than the one with vertical reinforcement only. The horizontal reinforcement acts as a secondary flexural reinforcement. The beam with both horizontal and vertical web reinforcement responds even stiffer. Plots with the principal tensile strains show that the use of a bi-directional mesh prevents localization of strains and thus large deformations.

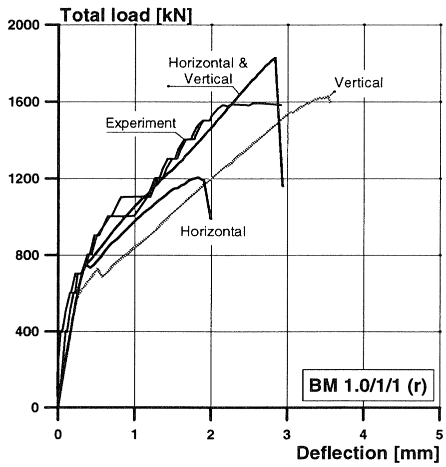

Fig. 10. Load-deflection diagrams for BM 1.0/1/1 (r) with varying orientation of web reinforcement.

The orientation of the web reinforcement also has an influence on the load distribution. The fact that a horizontal reinforcement acts as a secondary flexural reinforcement results in a smaller load transfer towards the inner support: the behaviour tends towards that of a single span beam, as becomes clear from the relative support reaction (Table 4).

Figure 11 shows the effect of the orientation of the web reinforcement on the final crack pattern. Only crack widths larger than 0.05 mm are shown.

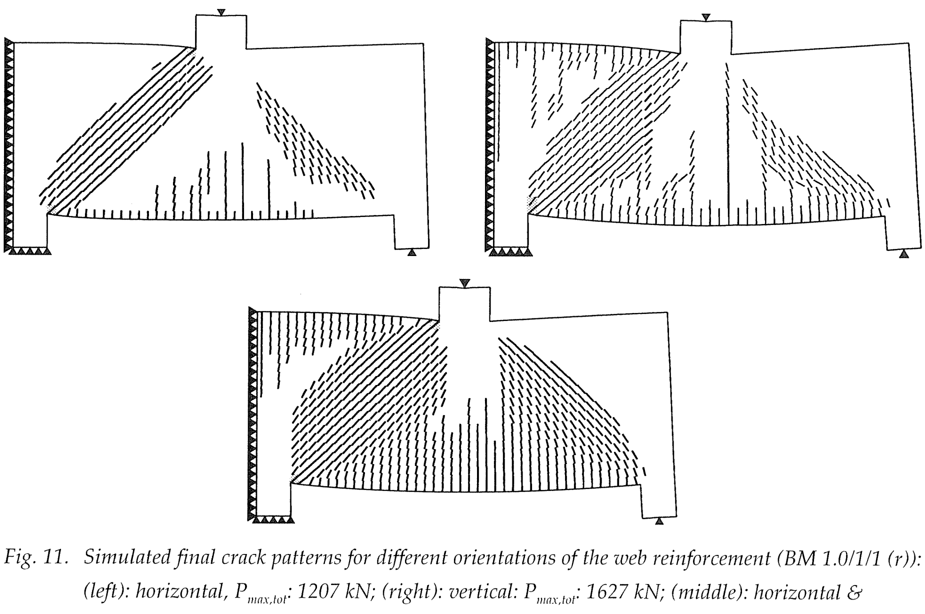

Fig. 11. Simulated final crack patterns for different orientations of the web reinforcement (BM 1.0/1/1 (r)): (left): horizontal, $P_{max,tot}$: 1207 kN; (right): vertical: $P_{max,tot}$: 1627 kN; (middle): horizontal & vertical, $P_{max,tot}$: 1827 kN.

It reveals that application of *both* vertical and horizontal web reinforcement results in a very diffuse crack pattern. Almost no localization can be seen, because a relatively uniform strain field (with small strains) prevails. If the web reinforcement is oriented in one direction, a more or less well defined shear crack band is detected. In the case of horizontal reinforcement only, the final crack pattern also suggests that the top reinforcement is not fully utilized. At this ultimate !! loading stage *no cracks* larger than 0.05 mm can be detected in the vicinity of the longitudinal reinforcement.
The failure mode remains unaffected: failure occurs by crushing of the concrete in the areas adjacent to the loading column and the middle support.

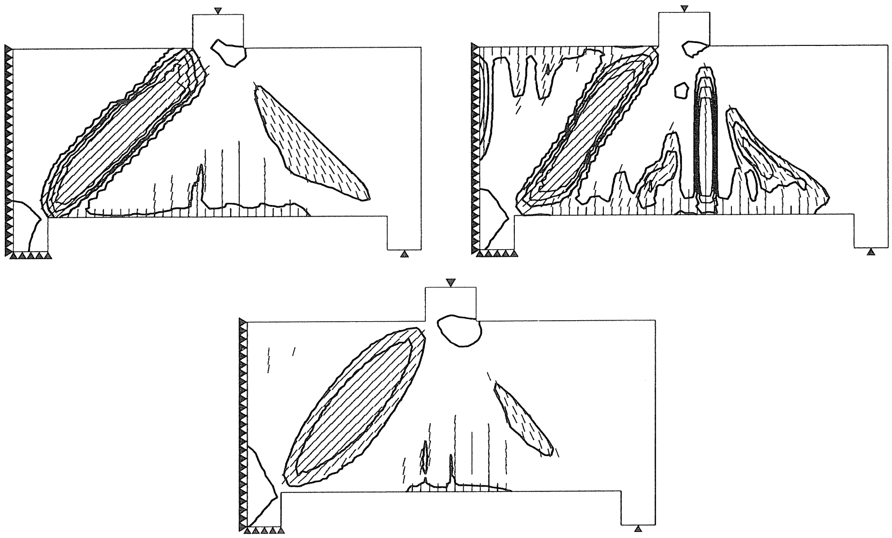

Fig. 12 Isolines for principal tensile strains at 1200 kN total load for different orientations of the web reinforcement (BM 1.0/1/1 (r)): (left): horizontal; (right): vertical; (middle): horizontal & vertical.

Figure 12 presents the isolines for principal tensile strains for BM 1.0/1/1 (r) for different orientations of web reinforcement.
It is shown that localization of strains in the shear span only occurs if the web reinforcement is placed in one direction. If a bi-directional mesh of reinforcement is used, tensile strains (read: crack widths) are smaller and more uniform. The isolines support the observation that in the case of horizontal web reinforcement only, the top reinforcement is not fully utilized.

5 Conclusions

This paper shows that non-linear finite element analysis of reinforced concrete continuous deep beams can be used complementary to experiments.

The simulations provide additional insight into the structural behaviour. The experimental tendencies are well predicted. This concerns both overall structural behaviour (e.g. crack pattern development, load-deflection response), and local structural behaviour (change in internal load transfer due to shear cracking).

Once a sufficiently accurate relation between experiment and simulation has been established, extrapolation is possible by simulating the behaviour beyond the tested range. For this purpose both a material and a structural parameter were varied.

The influence of a *material* parameter, namely the reduction of the compressive strength due to transversal tensile strains, on the structural response was investigated.
Only for large reductions of the compressive strength a change in failure mechanism as well as a decrease of the ultimate load was found. In all other cases, no significant influences could be detected on either overall or local structural response.

The influence of a *structural* parameter, namely the amount and the orientation of web reinforcement, on the ultimate shear strength was also investigated.
Compared to the calculation with vertical reinforcement only, the simulation showed a decrease in shear strength when only horizontal reinforcement is used. The horizontal reinforcement acts as supplementary flexural reinforcement. A combination of both horizontal and vertical reinforcement is the most effective way to increase the shear strength, albeit at the expense of more reinforcement. Additionally, crack widths are limited. Therefore, the use of well distributed web reinforcement in two directions is recommended for practical purposed. The simulations validated the choice made in the experimental programme.

The results of both the experimental and the numerical investigations have led to better insight into the structural behaviour of reinforced concrete continuous deep beams. This can be used to formulate better rules for design and more rational design models.

6 Acknowledgements

The authors like to thank Mr. F. Schilperoort and Mr. A van Rhijn for carrying out the experiments, Dr. Cervenka and Dr. Pukl for their support with the numerical simulations, and Ir. A. Vervuurt for his expertise on the PostScript-language.

7 References

American Concrete Institute (1989). "Building Code Requirements for Reinforced Concrete." ACI318-89, American Concrete Institute, Detroit, 1989.

Asin, M. (1992). Behaviour of Statically Indeterminate Deep Beams. *Progress in Concrete Research*, Vol. 3, Delft University of Technology, pp.45-58.

ASIN, M., WALRAVEN, J. C. and CERVENKA, V. (1994), Reinforced Concrete Continuous Deep Beams: Numerical and Experimental Behaviour, In *Proceedings Computer Modelling of Concrete Structures*, (eds. H. Mang, N. Bićanić and R. de Borst), Pineridge Press, Innsbruck, Austria, pp.713–722.

BAŽANT, Z. P. and OH, B. H. (1983), Crack Band Theory for Fracture of Concrete, *Materials and Structures* **93**(13): pp.155–177.

CERVENKA, V., ELIGEHAUSEN, R. and PUKL, R. (1990). "SBETA Computer Program for Nonlinear Finite Element Analysis of Reinforced Concrete Structures." 1990/1, Universität Stüttgart – Institut für Werkstoffe im Bauwesen, November 1989.

CERVENKA, V. and PUKL, R. (1992), Computer Models for Concrete Structures, *Structural Engineering International* **2**(2): pp.103–107.

CERVENKA, V. and PUKL, R. (1993), SBETA Analysis of Size Effect in Concrete Structures, In *Proceedings Size Effect in Concrete Structures*, (eds. H. Mihashi, H. Okamura and Z. P. Bažant), E&FN Spon, Sendai, Japan, pp.323–333.

Commission of the European Community (1991). "EuroCode 2 - Design of Concrete Structures – Part 1: General rules and rules for buildings." ENV 1992-1-1, 1991.

CSA (1984). "Design of Concrete Structures for Buildings." CAN3-A23.3-M84, Canadian Standards Association, December 1984.

FEENSTRA, P. H. (1993). "Computational Aspects of Biaxial Stress in Plain and Reinforced Concrete." Dissertation, Delft University of Technology.

HORDIJK, D. A. and REINHARDT, H. W. (1990), A constitutive model for crack cyclic behaviour of plain concrete, In *Proceedings Fracture Behaviour and Design of Materials and Structures*, (ed. D. Firrao), EMAS, Torino, Italy, pp.579–584.

KOLLEGGER, J. and MEHLHORN, G. (1990). "Experimentelle Untersuchungen zur Bestimmung der Druckfestigkeit des gerissenen Stahlbetons bei einer Querzugbeanspruchung." Heft 413, Deutscher Ausschuss für Stahlbeton, 1990.

KOLMAR, W. (1985). "Beschreibung der Kraftübertragung über Risse in nichtlinearen Finite-Element-Berechnungen von Stahlbetontragwerken." Dissertation, Technischen Hochschule Darmstadt.

KONG, F.-K., ROBINS, P. J. and COLE, D. F. (1970), Web Reinforcement Effects on Deep Beams, *ACI Journal* **67**(12): pp.1010–1017.

LEHWALTER, N. (1988). "Die Tragfähigkeit von Betondruckstreben in Fachwerkmodellen am Beispiel von gedrungenen Balken." Dissertation, Technischen Hochschule Darmstadt.

MAU, S. T. and HSU, T. T. C. (1987), Shear Strength Prediction for Deep Beams with Web Reinforcement, *ACI Structural Journal* **84**(6): pp.513–523.

ROGOWSKY, D. M. (1990). Continuous Deep Beams. Reinforced Concrete Deep Beams, Blackie / Van Nostrand Reinhold, F. K. Kong ed., pp.95–114.

ROGOWSKY, D. M. and MacGregor, J. G. (1983). "Shear Strength of Deep Reinforced Continuous Deep Beams." Structural Engineering Report No. 110, University of Alberta, Edmonton, November 1983.

SMITH, K. N. and VANTSIOTIS, A. S. (1982), Shear Strength of Deep Beams, *ACI-Journal* **79**(3): pp.201–213.

VECCHIO, F. J. and COLLINS, M. P. (1983). "The Response of Reinforced Concrete to In-Plane Shear and Normal Stresses." Publication No. 82-03, University of Toronto, Department of Civil Engineering, March 1982.

VECCHIO, F. J. and COLLINS, M. P. (1993), Compression Response of Cracked Concrete, *ASCE Journal of Structural Engineering* **119**(12): pp.3590–3610.